AMERICAN JOURNAL OF PHYSICAL ANTHROPOLOGY 157:571–581 (2015)

# Analysis of the Human Osseous Nasal Shape—Population Differences and Sexual Dimorphism

Stefan Schlager* and Alexandra Rüdell

*Department of Anthropology, University of Freiburg, Baden-Württemberg, Germany*

*KEY WORDS* geometric morphometrics; cranial morphology; human variation

*ABSTRACT* *OBJECTIVES:* In this study, the shape of the outer osseous nose in a German and a Chinese sample is analyzed using a dense set of semi-landmarks. Shape differences related to population and sex as well as directional and fluctuating asymmetry were statistically evaluated and also visualized.
*MATERIALS AND METHODS:* Shape differences in the bony nose were investigated between a large sample of CT scans of German (140 ♀, 127 ♂) and Chinese (135 ♀, 132 ♂) crania. We used semi-automatic methods to represent the shape of this region as a dense point-cloud, consisting of 370 three-dimensional bilateral coordinates. Both the symmetric and asymmetric modes of shape variation were addressed.
*RESULTS:* Strong differences in nasal shape were found between the two populations, while sex was found to play a minor role in explaining the observed shape variation. The expression of sexual dimorphism was similar in both populations. Differences attributed to population affinity and to sexual dimorphism were both found to affect the shape of the *ossa nasalia* and the projection of the *spina nasalis*. The correlation with population/sex was weak for directional asymmetry, but strong for fluctuating asymmetry. The nasal region is more asymmetric in Germans than in Chinese, with males displaying more asymmetry than females in both populations.
*DISCUSSION:* While the bony nose is well suited for predicting population affinity, regarding the populations under investigation, its value for sexing unknown individuals is rather moderate. The similar expression of sexual dimorphism in those otherwise very dissimilar populations indicates common factors responsible for these differences. Am J Phys Anthropol 157:571–581, 2015. 

The shape of the human osseous nose, and its variation between populations and sexes, is of great importance in scientific fields such as evolutionary, physical, and forensic anthropology.

Because the shape of the osseous nose has adapted to different climates it is highly dependent on geographic region (Franciscus and Long, 1991; Yokley, 2009; Butaric et al., 2010; Noback et al., 2011; Holton et al., 2013; Evteev et al., 2014). It is therefore often analyzed to determine the population affinity of unknown individuals, preferably together with other craniofacial features (Jantz and Ousley, 2005; Sholts et al. 2011). Shape analysis of the osseous nose can also help with population-specific sex estimation, both when analyzing the nose as an isolated structure (Bigoni et al., 2010) and in combination with other features (the preferred approach) (Birkby, 1966; Kimmerle et al., 2008; Bigoni et al., 2010; Humphries and Ross, 2011; Franklin et al., 2013; Ogawa et al., 2013). Closely related to sexual dimorphism is the influence of allometry due to sex-specific differences in size (Rosas and Bastir, 2002; Kimmerle et al., 2008) and asymmetry (Gangestad and Thornhill, 2003; Claes et al., 2012).

While directional asymmetry is likely linked to genetic (Kimmerle and Jantz, 2005) and ontogenetic factors, e.g. mechanical loading during growth (Özener, 2010), fluctuating asymmetry can be seen as indicator for developmental instability (Gangestad and Thornhill, 2003; Graham et al., 2010). Fluctuating asymmetry therefore reveals how well an organism copes with environmental stress (Penton-Voak et al., 2001), and is puportedly linked to sexual attractiveness and mating choices (Penton-Voak et al., 2001; Koehler et al., 2004). Thus, while symmetry analysis may not necessarily help with sexing or identification of unknown human remains, nose symmetry can provide information on the disease and life history of an individual. From an evolutionary perspective, it is of interest to examine symmetry variation on a population level. Most studies on asymmetry of the human face analyze the soft tissue, because as a visible feature, it influences facial attractiveness (Gangestad and Thornhill, 2003). However, we have previously shown that asymmetric effects visible in the soft tissue nose can be linked to asymmetry present in the underlying bone tissue (Schlager, 2012).

From a methodological point of view, most studies on the osseous nose employ linear measurements (Glanville, 1969; Yokley, 2009; Evteev et al., 2014). Some recent studies have used geometric morphometrics to analyze sets of anatomical landmarks (Kimmerle et al., 2008; Noback et al., 2011; Bastir and Rosas, 2013). One advantage of geometric morphometrics over traditional methods is the possibility to investigate size and shape of a structure separately (Adams et al., 2004; Slice, 2005; Mitteroecker et al., 2013). This is especially important for detailed analyses on the interaction between sexual dimorphism and allometry (Rosas and Bastir, 2002). Using a dense set of semi-landmarks (Bookstein, 1997; Gunz et al., 2005) furthermore allows detection of subtle variation in shape which is not observable using

*Correspondence to: Stefan Schlager, University of Freiburg, Anthropology, Hebelstr 29, Freiburg, 79104, Germany.
E-mail: stefan.schlager@uniklinik-freiburg.de

Received 5 June 2014; accepted 14 March 2015

DOI: 10.1002/ajpa.22749
Published online 6 April 2015 in Wiley Online Library (wileyonlinelibrary.com).

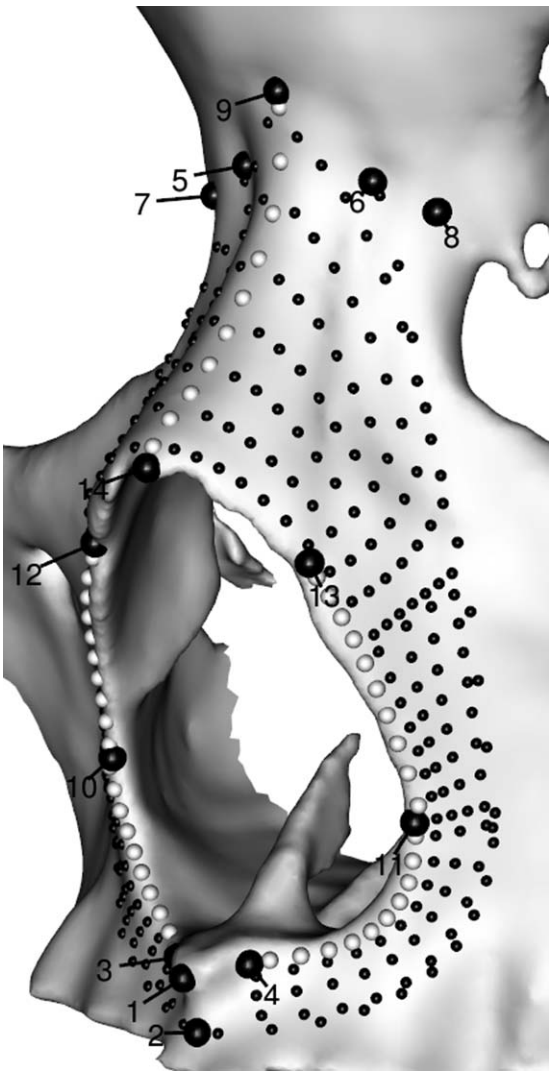


**Fig. 1.** Coordinates defining bony nose shape. Manually placed landmarks (large black spheres) semi-landmarks defining curves (gray medium-sized spheres) and surfaces (small black spheres).

only anatomical landmarks (Hennessy et al., 2005; Claes et al., 2012; Gunz and Mitteroecker, 2013). This approach also reduces observer error (Schlager, 2013) and enhances the possibilities of visualization (Gunz and Mitteroecker, 2013).

In this work, we compare shape differences in the osseous nose of a large sample of modern male and female Chinese and Germans. As studies on the osseous nose typically focus on different subregions, we here focus on the osseous tissue of the outer nose (Fig. 1), further referred to as "the bony nose." The analysis is based on a data set of medical computed tomography (CT) 3D models of skulls, which are investigated via 3D-geometric morphometrics using anatomical landmarks supported by a dense set of semi-landmarks. A major goal of the article is to investigate the discriminatory power of such an approach. In addition, this study provides detailed analyses and illustrations of population-specific shape differences regarding the bony nose, based on large German and Chinese samples. A particular question that we address is whether there is a correlation between fluctuating asymmetry and the generally more projected nose in Germans: if asymmetry is dependent on the specific shape of a structure, this has to be taken into account when comparing asymmetry between populations. Overall, the modes of variation presented, including size-corrected population differences in sexual dimorphism and asymmetry, are not only useful for scholars working with these regional populations, but also provide baseline data on the variation present in specific groups.

## MATERIAL AND METHODS

### Sample

The material studied consists of 534 computed tomography (CT) scans taken in the course of medical treatment in two hospitals: the *University Medical Centre Freiburg* and the *Ninth Peoplés Hospital, Shanghai*. The data are anonymized, with age, sex, and population affinity being the only information available. Population affinity refers to the place of the hospitals where the CT scans were acquired (Freiburg or Shanghai), so we do not have information about the exact ancestry but refer to "German" and "Chinese" population affinity accordingly. Homogeneity with respect to provenance cannot be guaranteed, but naturally most patients come from the areas surrounding the hospitals. One major advantage of a large sample size is that the majority of relatively homogeneous data outweighs a few outliers.

Only adult individuals (>18 years) with no signs of pathologies in the facial region were included in the analysis. The data are almost equally distributed regarding population affinity and sex, consisting of 267 Germans (140 ♀, 127 ♂) and 267 Chinese (135 ♀, 132 ♂). The average age is 43.2 years for Chinese female, 45.7 years for Chinese males, 50.6 years for German females, and 48.7 years for German males.

### Data acquisition

Triangular surface meshes, representing the bony nose, were generated from the CT-data utilizing the software program Voxim®.[1] 14 anatomical landmarks (Fig. 1), defined in Table 1, were then placed on these surface meshes.

Additionally, three curves were manually placed on the surface representations of all individuals using the software program Landmark v.3.6.[2]

Two of these curves represent the nasal aperture, connecting *nariale*, *alare*, and *nasomaxillare*, while the third runs along the ridge on the back of the nasal bones in a straight line between *nasion* and *rhinion* (Fig. 1), roughly following the sutura internasalis. Semi-landmarks defining the surface surrounding the nasal aperture and the *ossa nasalia* were defined on a reference individual and then projected onto all other surfaces applying the routines described in Schlager (2013, pp. 37–40) and utilizing the R-package Morpho (Schlager, 2014). The implemented regularization ensures the correct positioning of the surface patches by comparing surface topology and subsequent relaxation against the template configuration. Landmarks and semi-landmarks were placed bilaterally, where suitable. To guarantee mathematical homology for semi-landmarks, they were allowed to slide along the

[1]http://www.ivs-technology.de/en/products.php

[2]http://graphics.idav.ucdavis.edu/research/EvoMorph

*TABLE 1. Definition of cranial landmarks (Numbers correspond to Fig. 1)*

| No. | Landmark | Description |
|---|---|---|
| 1 | *Nasospinale* | Tip of *spina nasalis anterior* |
| 2 | *Subspinale* | Transition of frontal downward edge of the *spina nasalis anterior* into the *processus alveolaris*. |
| 3/4 | *Nariale* | Beginning of the transition of the lower border of the a*pertura nasalis* into the structure of the n*asospinale* |
| 5/6 | *Nasomaxillofrontale* | Intersection of *sutura frontonasalis* and *sutura nasomaxillaris* |
| 7/8 | *Maxillofrontale (modified)* | Intersection of *sutura frontomaxillaris* and the *Anterior lacrimal crest*. If not clearly visible, this is estimated by the point on the suture closest to the point where the orbital rim flattens |
| 9 | *Nasion* | Intersection of *sutura internasalis* and *sutura frontonasalis* |
| 10/11 | *Alare* | Most lateral positions of the *apertura nasalis* (taken in frontal view) |
| 12/13 | *Nasomaxillare* | Distal endpoint of the *sutura nasomaxillaris* |
| 14 | *Rhinion* | Median most downward endpoint of the *sutura internasalis* (as the latter is mostly invisible, the most downward point is used) |

*TABLE 2. Results of Procrustes ANOVA testing for fluctuating asymmetry based on 37 observer tested specimens*

| Factor | SS | MS | df | *F* | *P*-value |
|---|---|---|---|---|---|
| ind | 1.541 | $6.775 \times 10^{-5}$ | 22,752 | 16.421 | $<10^{-16}$ |
| side | 0.004 | $6.503 \times 10^{-6}$ | 630 | 1.576 | $<10^{-16}$ |
| ind × side | 0.094 | $4.125 \times 10^{-6}$ | 22,680 | 7.341 | $<10^{-16}$ |
| error | 0.079 | $5.619 \times 10^{-7}$ | 140,082 | – | – |

The factor *ind* refers to variation explained by individual variation, *side* to directional asymmetry, *ind* × *side* to fluctuating asymmetry and *error* to the observer error. The significance of the term *ind* × *side* indicates the presence of a significant amount of fluctuating asymmetry.

surface and curves, minimizing bending energy towards the sample's average (Gunz et al., 2005). A regularization by relaxation against a symmetrized average, as outlined in Schlager (2012, 2013, pp. 36, 37), was applied to remove asymmetry not inherent in the individual shapes but, for example, induced by the patch placement algorithm. This allows the assessment of symmetric and asymmetric variation in semi-landmark configurations applying methods that are already well established in statistical shape analysis based on traditional landmark configurations (Klingenberg and McIntyre, 1998; Mardia et al., 2000; Klingenberg et al., 2002). Since error testing proved *nasomaxillare* (12, 13) and *alare* (10, 11) to be prone to inter- and intraobserver error (Schlager, 2013, pp. 44–47), they were subsequently treated as semi-landmarks and included in the sliding process to reduce variation due to observer error (for details see Schlager, 2013, pp. 42–47). Our total dataset consists of 10 craniometric landmarks, 54 semi-landmarks on three curves and 306 semi-landmarks interpolating the surface shape, totaling 370 3D-coordinates that were included in the analysis.

## Data analysis

All analyses were carried out utilizing the statistical platform R (R Development Core Team, 2011) and specifically the R-package Morpho (Schlager, 2014).

***Preliminaries.*** Preceding the statistical analyses, a full General Procrustes Analyses (GPA) (cf. Goodall, 1991; Dryden and Mardia, 1998) for data with object symmetry was performed (Klingenberg and McIntyre, 1998; Klingenberg et al., 2002). The outcome is composed of a symmetric and an asymmetric shape component. The symmetric shape component is defined as the consensus between the superimposed original and mirrored landmarks. The deviations from this symmetrized configuration constitute the asymmetric component. As shown by Mardia et al. (2000), the resulting subspaces of the shape space are orthogonal and can be evaluated separately. In general, one can assume that the symmetric shape component contains the overall shape variability. The asymmetric shape component can be analyzed as a specific type of shape variation, which permits testing for the presence and intensity of asymmetry, as well as detailed visualization of the associated shape differences. The existence of a significant amount of directional asymmetry was tested using Procrustes ANOVA (Klingenberg et al., 2002). For testing whether fluctuating asymmetry can be separated from observer error, landmarks, and curves where digitized twice by two observers on 37 randomly selected specimens. Procrustes ANOVA then was calculated in order to test for statistical significance of fluctuating asymmetry, showing fluctuating asymmetry to be highly significant (Table 2).

The data resulting from the GPA consist of 1110 variables per specimen (370 3D-coordinates) which greatly exceeds sample size. We applied principal component analysis (PCA) to reduce data dimensionality. Subsequent statistical tests were run on the principal components (PCs) accounting for at least 95% of the sample's overall variation. These are 13 PCs, accounting for 95.1% of the symmetric variance and 21 PCs explaining 95.0% of the asymmetric shape variance.

Q-Q-plots indicated multivariate normality for the symmetric shape component and a strong long-tail deviation for the asymmetric shape component, suggesting that parametric tests on the asymmetric shape component should be interpreted with caution and additional nonparametric testing procedures, such as permutation testing, should be applied. In this study, all permutation tests were run with 10,000 rounds.

***Assessing population differences.*** For assessing differences of bony nose shape between populations, we applied a variety of parametric and nonparametric testing procedures, both for the symmetric and the asymmetric shape component.

Population differences concerning the symmetric shape were modeled by a linear regression model based

on the first 13 symmetric PCs against the factor *population*. Significance of group differences was assessed using 50–50 MANOVA and permutation testing.

50–50 MANOVA (Langsrud, 2002; Langsrud et al., 2007) is a modified version of a standard MANOVA, designed for many (potentially correlated) response variables. The algorithm also allows for the avoidance of variable scaling to unit variance, thus maintaining the importance of each principal component within the sample in question. In that case, other than in a standard MANOVA, the sums of errors are not calculated from standardized variables, resulting in generalized distances, but rather display Euclidean distances in shape-space. This leads to more cautious results when claiming significance because very small differences, possibly apparent among less important (for the sample structure) variables, are weighted down. We applied 50–50 MANOVA with and without standardization using the R-package *ffmanova* (Langsrud and Mevik, 2012).

Additionally, we ran permutation tests to double check the results without assuming a specific probability distribution or equal covariance matrices. Hereby, the differences measured between groups are compared to those calculated from 10,000 random regroupings and a *P*-value is calculated by dividing the number of random values exceeding the actual measurement by the number of permutations.

Standard discriminant function analysis (DFA) was applied for classification purposes and the classification accuracy is estimated by conducting a leaving-one-out cross-validation. Because DFA requires equal covariance matrices in all groups, we first assessed differences in covariance structure. This was done by obtaining the pairwise (Riemannian) distances between the group-specific covariance matrices and testing their significance by permuting over the grouping variable (10,000 rounds) (Mitteroecker and Bookstein, 2009). In case of differing covariance matrices, we additionally applied a between-group PCA (between-group PCA) for classification, as this procedure does not rely on similar covariance matrices, at the cost of a lower discriminatory power. Hereby, all variables are projected into the eigenspace of the between-group covariance matrix, resulting in a low dimensional representation of the between-group structure (Boulesteix, 2005; Mitteroecker and Bookstein, 2011).

Group differences concerning asymmetry were assessed by 1) shape and 2) amount of asymmetry. Population specific shape differences were analyzed using multivariate testing procedures based on the first 21 PCs derived from the asymmetric component, using 50–50 MANOVA and permutation testing. Within the asymmetric subspace, the direction of each shape vector can be interpreted as direction of asymmetric displacement and its length as amount of asymmetry, i.e., how far away the shape is from a perfectly symmetric configuration (for details see Schlager, 2013, pp. 67–69).

Because the direction of asymmetry is given by the direction of the respective shape vector, population differences can be calculated as angle between their average asymmetric shape vectors. Its significance was assessed by comparing the actual angle to those obtained from 10,000 random regroupings. For estimating the amount of fluctuating asymmetry in each population, we first subtracted the population-specific directional asymmetry from each configuration (Krajíček et al., 2012) and then calculated both the Euclidean vector length as well as the squared Mahalanobis distance of the remaining asymmetric deviation. As both variables exhibit a log-normal distribution, ANOVAs are calculated on the log-transformed data.

***Assessing sexual dimorphism.*** Because sexual dimorphism does not only affect shape but also size (Rosas and Bastir, 2002; Kimmerle and Ross, 2008), we considered allometric effects when dealing with shape differences associated with sex. As a measure of size we chose centroid size (CS). The significance of sexual dimorphism regarding size was assessed by ANOVA testing on the linear model "*centroid size against population* × *sex*".[3]

To test for common allometry, we applied 50–50 MANOVA testing on the linear model regressing the group-centered PC-scores of the symmetric shape component against centroid sizes. Additionally, we calculated the common allometric scores (Mitteroecker et al., 2004). To minimize allometric effects, common allometry was removed from the data: First, shape data and centroid sizes were corrected for *population* and *sex* by centering on group averages. These data were then used to calculate the linear regression model "*shape against CS*". Finally, the residuals of this model were readded to the groups' averages, resulting in data with the common allometric trend stripped off.

Similar to the above outlined procedure of analyzing population differences, we assessed the significance of between-group distances and used permutation testing to further analyze the interaction between shape as response variables and *population* and *sex* as predictors. We modeled population-specific sexual dimorphism as shape vectors connecting male and female averages in both populations. This way, the interaction between population affinity and sexual dimorphism can be understood as differences in length and direction of these shape vectors. The Euclidean vector norm (i.e., length of a vector) refers to the intensity of sexual dimorphism and the difference in direction, calculated as angle between those vectors, can be interpreted as difference between shape patterns, associated with population specific sexual dimorphism (Adams and Collyer, 2009).

The significance of each value was calculated by permutation testing. To achieve this, the data were corrected for population differences and the measured vector properties, associated with sexual dimorphism, were compared to those calculated from data with randomly reassigned population affinity (Schlager and Metzger, 2011).

Sexual dimorphism concerning the asymmetric shape component was assessed by the same methods used to analyze population differences.

## RESULTS

### Population differences

***Symmetric variation.*** Statistical analyses on the first 13 PC-scores of the symmetric shape component produced the following results. The variance associated with the linear model "*shape against population affinity*" explained 32.4% of overall shape variation (50–50 MANOVA: $P < 2 \times 10^{-16}$, Permutation testing: $P < 0.0001$).

[3]The '×' denotes the inclusion of an interaction term.

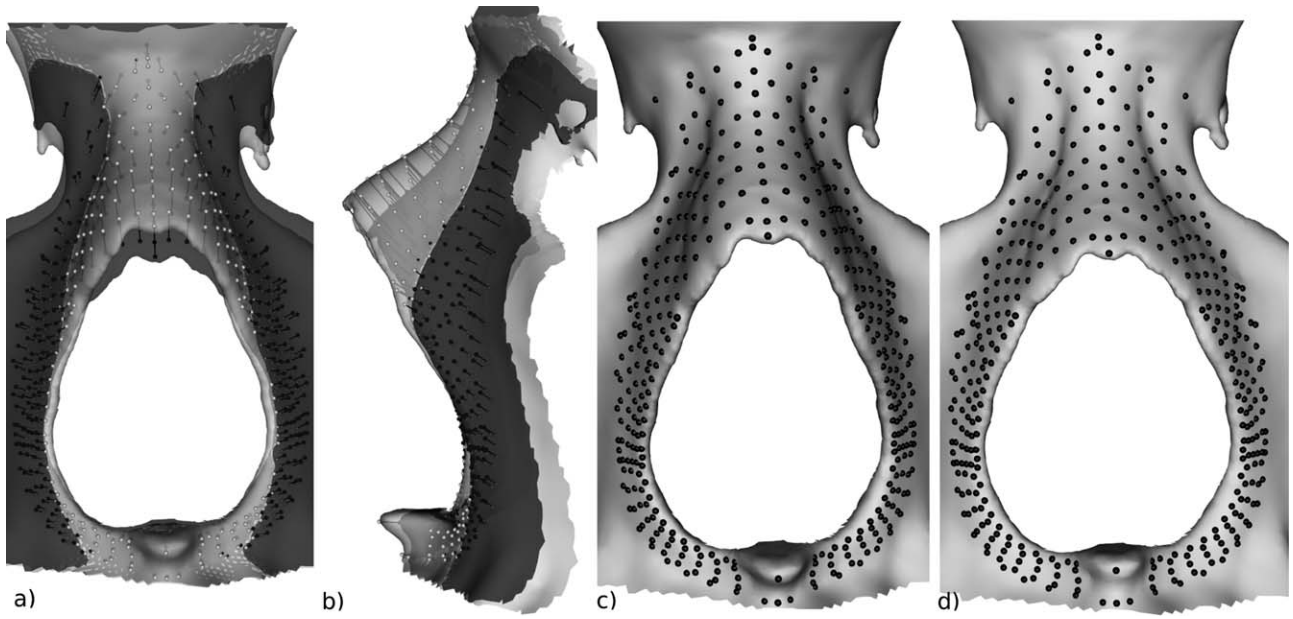


**Fig. 2.** Surface meshes warped to landmark configurations of population averages (light gray: German; dark gray: Chinese) of the symmetric shape component in frontal (**a**) and lateral view (**b**). (**c**) shows the average German shape and (**d**) the average Chinese.

*TABLE 3. Results of procrustes ANOVA testing for directional asymmetry*

| Factor | SS | MS | exVar | df | *F* | *P*-value |
|---|---|---|---|---|---|---|
| ind | 3.093 | 0.00001 | 0.875 | 297,414 | 7.395 | $<10^{-16}$ |
| side | 0.033 | 0.0001 | 0.009 | 545 | 43.443 | $<10^{-16}$ |
| ind × side | 0.408 | 0.00000 | 0.116 | 290,485 | – | – |

The factor *ind* refers to variation explained by individual variation, *side* to directional asymmetry and *ind* × *side* to fluctuating asymmetry. The column *exVar* reports an estimation of the variance explained by this factor.

Crossvalidated DFA produced a correct classification rate of 97.4% for Chinese and 97.0% for Germans (with the overall accuracy being 97.2%). As covariance matrices between populations differed significantly ($P = 0.0001$), we double-checked this result by calculating a between-group PCA, using population affinity as grouping variable. The resulting accuracy was slightly lower with a correct classification of 96.1% for Chinese and 93.8% for Germans. To visualize population-specific differences (Fig. 2), a surface mesh was warped to population averages by a thin-plate spline (TPS) deformation (Bookstein, 1989). The strongest differences were found in the shape of the *os nasale*, that is more projected in Germans. In lateral view, the distance between *nasion* and *maxillofrontale* is much larger in Germans. The use of a dense set of semi-landmarks allowed several observations, which are not detectable using single landmarks or even linear measurements, outlined in the following. The *spina nasalis* is more prominent in Germans, but with a similar inclination in both populations. The shape of the *apertura piriformis* is more elongated in Germans compared to the wider and more roundly shaped mean shape of the Chinese sample. Changes in curvature of the nasal bones' profile between *rhinion* and *nasion*; however, are similar in both populations, being concave in the upper part and convex towards *rhinion*.

In addition, the saddle made up by the nasal bones is broader in the German mean shape than in the Chinese (Fig. 2). Looking at the region around the *spina nasalis* in Figure 2 one can clearly see a more forward pointing *spina nasalis* in Germans and also a slightly forward moved region around both left and right nariale. When following the course of the rim of the piriform aperture from *spina nasalis* to *rhinion*, it can be seen that the narrowing of the aperture in Germans only starts after turning from horizontal to vertical direction. The shape of the base of the piriform aperture below this turning point is nearly the same in horizontal direction in both populations.

***Asymmetric variation.*** Procrustes ANOVA testing confirmed the presence of sample-wide directional asymmetry (Table 3). Despite being highly significant ($P < 1 \times 10^{-18}$), its effect size is very small compared to the fluctuating asymmetry (Table 2, column "exVar"). For testing population differences concerning directional asymmetry, we took into account the first 21 PC-scores of the asymmetric shape component. 50–50 MANOVA including standardization reports very high significance ($P = 3.5 \times 10^{-15}$). Without standardization the *P*-value increases to 0.000339. The factor *population* accounts for 0.6% of the asymmetric variance. As Q-Q-plots indicated a significant deviation from normality for the asymmetric shape component, we double-checked the result with permutation testing. The latter reported significance with a *P*-value of 0.0151. To test whether this significance results from the intensity or the direction of asymmetry, we conducted permutation tests as outlined above. While the intensity of directional asymmetry is similar in both populations ($P = 0.9933$), the direction differs significantly ($P = 0.0063$) by 31.2°. For visualization purposes, we exaggerated the population specific asymmetry by factor 10. Figure 3 shows a leftward trend for the nasal bones and an opposing direction of asymmetry in the lower parts of the *apertura piriformis* and the *spina nasalis in both populations*.

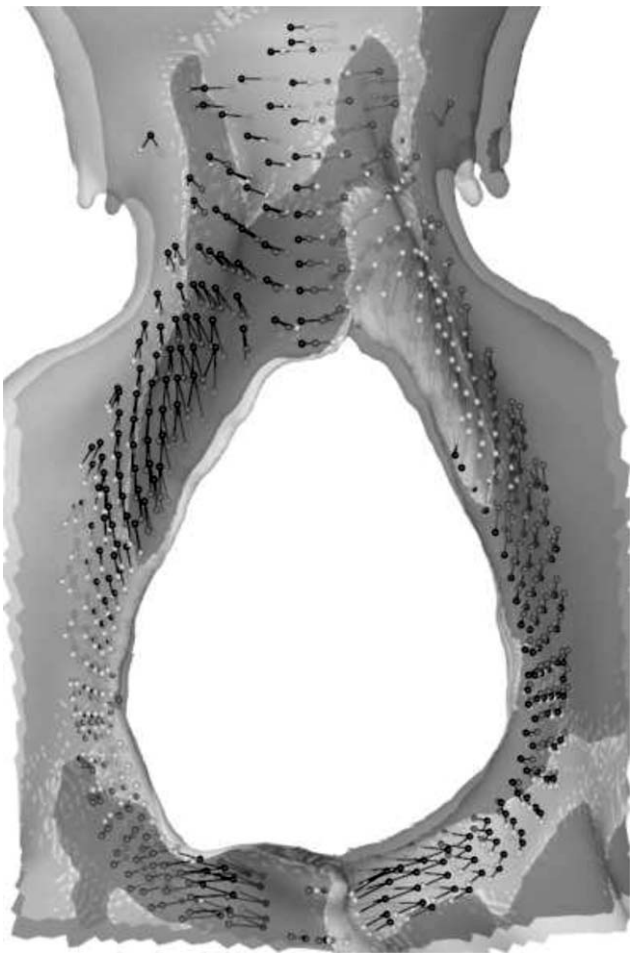

**Fig. 3.** Population specific directional asymmetry (exaggerated by factor 10) in frontal view. Light gray = Germans, dark gray = Chinese. Black spheres depict the symmetric overall consensus.

Additionally, we tested for differences in the amount of fluctuating asymmetry inherent in both populations. ANOVAs, calculated on the log-transformed Euclidean and squared Mahalanobis-distances, reported those to be highly significant. *P*-values are $3.03 \times 10^{-15}$ ($R^2 = 0.1081$) for the vector lengths and $2.2 \times 10^{-16}$ ($R^2 = 0.1267$) for squared Mahalanobis-distances. This indicates stronger individual asymmetry within the German population (Fig. 4).

## Sexual dimorphism

***Allometry.*** As is to be expected, males and females differ significantly regarding size: ANOVA testing proved sex to be the most important factor for centroid size variation ($P < 2.2 \times 10^{-16}$, explaining 34.1% of its variance). No significant interaction between *population* and *sex* was detected.

Tests for common allometry using 50–50 MANOVA including variable standardization yielded highly significant results ($P = 7 \times 10^{-7}$); however, without standardization the reported *P*-value of 0.333 was far from being statistically significant. This indicates that allometric effects are associated with variables of minor importance for the overall variability. Additionally, the common allometric scores were calculated. They showed a weak but significant correlation with centroid size ($r = 0.2$; $P = 2.76 \times 10^{-6}$), also indicating that allometric effects are small.

***Symmetric variation.*** After correction for common allometry, the data were regressed on *population* × *sex*. 50–50 MANOVA, both on standardized and unstandardized data, reported sex to be highly significant ($P < 2 \times 10^{-16}$) in both cases, with an estimated explained variance of 2.9% in the pooled sample and 4.4% corrected for population differences and a significant interaction term (standardized data: $P = 0.0093$; unstandardized data: $P = 0.0035$; explained variance = 0.3%). As this test does not tell whether the significance of the interaction term can be associated with differences regarding the strength of sexual dimorphism or the direction of shape differences, we calculated permutation tests on these values, comparing the lengths and angles of the vectors connecting the averages of each sex in both populations. As a result, the differences can be attributed to different directions (angle between vectors is 34.0°, $P = 0.0086$), with differences in the strength of sexual dimorphism being insignificant ($P = 0.64$). The differences mostly affect the shape of the nasal bones, which are more projected in males (Fig. 5). Similarly to the population differences, the dense set of semi-landmarks lead to the detection of more subtle differences than it would be possible with traditional methods. The area around the *spina nasalis* is slightly more pronounced among males, with females having an upward inclination, similar in both populations. The piriform aperture tends to be slightly narrower in males than in females.

The discriminatory power of sexual dimorphism in the nasal region, however, is rather weak. DFA determined the cross-validated sexing accuracy to be 69.1% in the pooled sample—72.3% in the Chinese sample and 72.7% in the German one.

However, because centroid size is strongly associated with sex, we re-evaluated the classification by calculating a DFA with centroid sizes added to the first 13 PC-scores of the symmetric shape component. This raised the cross-validated accuracy to 83.3% using pooled data. Applying the DFA on the populations separately gives accuracies of 84.6% for the Chinese data and 88.2% for the German sample.

***Asymmetric variation.*** Testing the relation between directional asymmetry and sexual dimorphism, a 50–50 MANOVA on unstandardized data as well as a permutation test (10,000 rounds) report insignificance (with $P = 0.32$ for 50–50 MANOVA and $P = 0.245$ for permutation testing). On standardized data, the *P*-value decreased to 0.004. For taking into account population-specific differences, we also calculated a permutation test on pairwise distances between all groups in the pooled sample leading to insignificant results concerning sexual dimorphism in directional asymmetry (separate perpopulation *P*-values were 0.3758 for the Chinese sample and 0.1787 for the German sample).

Standard two-way ANOVAs of the log-transformed deviation (Euclidean and Mahalanobis distances) with predictors *sex* × *population* showed the factor *sex* to be significant ($P = 0.001$ for log Euclidean distances and $P = 0.0004$ for log-Mahalanobis distances) with no significant interaction between both predictors (corresponding *P*-values are 0.712 and 0.633). This indicates more asymmetry in males within both populations.

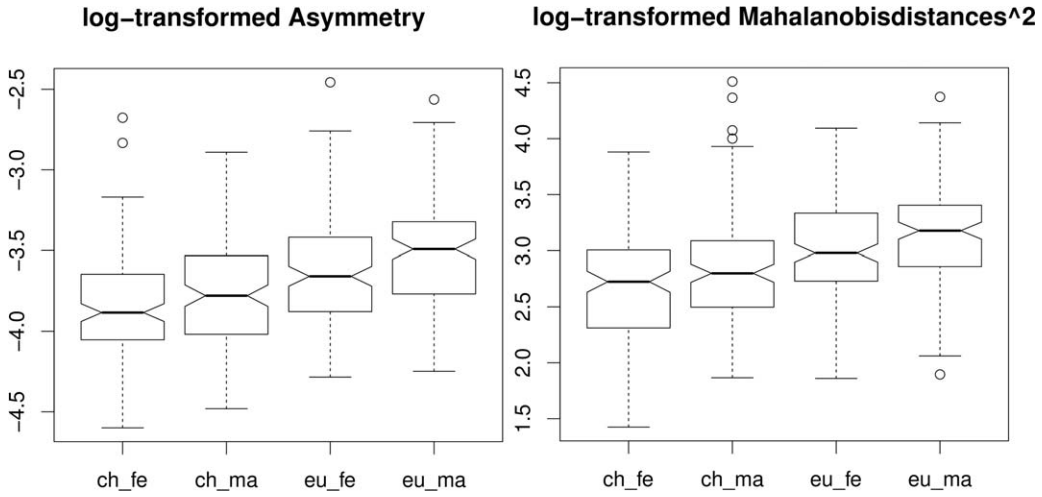


**Fig. 4.** Boxplots showing the amount of asymmetry inherent in the groups defined by population and sex. Left: log-transformed vector lengths; right: log-transformed squared Mahalanobis distances. Each figure displays from left to right: Chinese female, Chinese male, German female, German male. In both populations asymmetry is stronger in male and the German sample exhibit stronger asymmetry than the Chinese one.

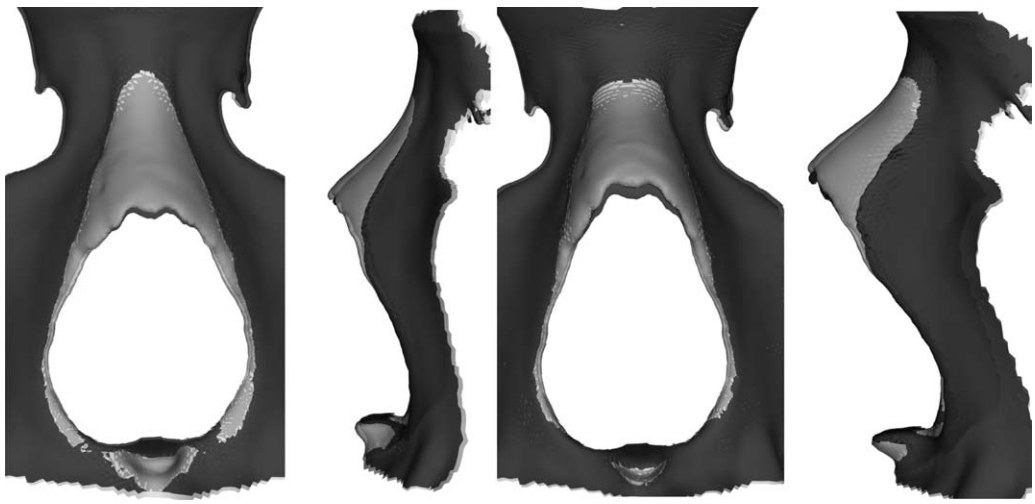

**Fig. 5.** Visualizations of population specific expression of sexual dimorphism. A surface is warped to the average shapes of the sexes in each population. Male and female are superimposed for each population with light gray surfaces depicting the male and dark gray surfaces showing female averages. It can be seen that the overall pattern of shape differences associated with sex are very similar in both populations. From left to right: Chinese in frontal view, Chinese in lateral view, Germans in frontal view, Germans in lateral view. Light gray = male; dark gray = female.

## DISCUSSION

In this study we looked at the shape variation of the bony nose in a sample of 534 individuals from China and Germany with respect to population affinity and sex under the aspect of the symmetric and asymmetric components of shape.

### Population differences

Our results show significant differences in the symmetric shape component of the bony nose between German and Chinese populations that allow a very accurate classification based on shape information. Population affinity was found to explain 32.4% of overall shape variation in our sample. The differences in shape are expressed by more upward pointing nasal bones and a more forward projected *spina nasalis* in Germans compared to Chinese, along with a slightly narrower piriform aperture. These differences lead to an elongated and, in relation to its height, narrower shape of the *apertura piriformis* in Germans. Our use of a dense set of semi-landmarks allowed detailed visualizations where these differences can be found (Fig. 5). The amount of shape information made it also possible to capture not only the different positions of single landmarks as in studies dealing solely with anatomical landmarks, but also to visualize that the curvature of the nasal bones is very similar in both populations. This led to the observation that the difference mainly lies in the angle the nasal bones constitute at *nasion*. The steepness of this angle, rather than the position of the lower part of the

nose, is responsible for a narrower or broader opening of the piriform aperture.

The between-population shape differences in the bony nose observed in our study are very distinct and yield excellent classification results. The shape variation in the nasal region might be related to climate, as found in earlier studies (Harvati and Weaver, 2006; Holton and Franciscus, 2008; Yokley, 2009; Noback et al., 2011; Bastir and Rosas, 2013; Evteev et al., 2014) but this was not explicitly tested in our study. The larger and more narrow nasal opening observed in the German populations confirms the shape found for populations living in cold and/or dry climates, whereas the smaller and more rounded nasal opening in the Chinese sample matches with warm and/or humid populations (e.g., Thomson and Buxton, 1923; Davies, 1932; Franciscus and Long, 1991; Hubbe et al., 2009; Noback et al., 2011; Evteev et al., 2014). Using our detailed method of registering the shape of the bony nose, future research, including detailed climatic information as well as a broader range of populations, can further improve our understanding of climatic adaptations in the nasal region.

When looking at asymmetric variation, we found significant differences concerning the directional asymmetry inherent in both populations. Despite its statistical significance and a difference of 31.2° between asymmetric shape vectors, directional asymmetry is very similar within both populations. It is expressed by a leftward movement of the nasal bones and a trend to the right at the lower part of the piriform aperture (Fig. 3). Keeping in mind that directional asymmetry is very subtle, it is still interesting to find this trend to be similar within the populations under study. While directional asymmetry is similar in intensity and direction, fluctuating asymmetry is stronger in the German sample. A possible explanation could be the more projected features of the nasal bones among Germans making them more prone to deformation. Comparisons to other populations, evaluating whether more prominent features can generally be associated with more asymmetry, might help to confirm this conjecture. If this was to be confirmed, future symmetry analyses should take this factor into account when explaining asymmetry between groups.

Generally, directional asymmetry is associated with mechanical load during bone growth as, for example, induced by handedness (Özener, 2010). When focusing on craniofacial asymmetry, it has been proposed that handedness and brain asymmetry may cause this, as well as mechanical loadings due to asymmetric chewing habits (Pirttiniemi, 1998). Also, in a study on human odor perception (Gilbert et al., 1989), handedness played a role in such that dextrals showed greater asymmetry between left and right nostrils concerning odor perception than sinistrals, but without preferring one specific nostril. Investigating this structural or functional asymmetry along the pathway from nostrils to the cortex, also the shape of the bony nose could be affected. In two of their samples, Bigoni et al. (2010) detected directional asymmetry in the nasal region similar to our findings, also stating a slight trend to the left of the upper part of the nasal bones and a rightwards displacement of the lower piriform aperture region. They interpret the pattern of directional asymmetry of the upper face as induced by mechanical loading due to a solid and gritty diet.

Concerning fluctuating asymmetry, measurement error might play some role (Palmer and Strobeck, 2003). But, as stated above, the amount of observer error is minimized by the use of a large amount of semi-landmarks. We furthermore showed that the fluctuating asymmetry is highly significant in our study when compared to observer error. Although fluctuating asymmetry has been widely discussed as an indicator for developmental instability, there are still more studies on the phenomenological aspects of fluctuating asymmetry than studies investigating the mechanisms concerning developmental instability (Klingenberg, 2003; Dongen, 2006). Our study does not allow conclusions about the nature of developmental instability, but it provides information about craniofacial fluctuating asymmetry in the way that it outweighs directional asymmetry concerning overall variability and is stronger in the bony nose of Germans than Chinese. Whether this difference is caused by higher developmental instability or by the aforementioned predisposition caused by the stronger protrusion of the bony nose in Germans can only be hypothesized at this point. To answer these questions, further research needs to be done concerning the concept of developmental instability as well as investigating craniofacial asymmetry in more populations.

## Sexual dimorphism

When focusing on shape differences in our sample, males exhibit more upward pointing nasal bones than females. In lateral view a slightly more convex shape is detectable for the lower part of male nasal bones (Fig. 5). The piriform aperture tends to be slightly narrower in males than in females. But the trend of an elongated aperture in males is also supported by the *spina nasalis* pointing a little more upwards in females. These shape differences lead to larger nasal cavities in males, which confirms previous studies on sexual dimorphism stating that males exhibit larger cranial airways due to increased airflow needs caused by higher energy expenditure (Bastir et al., 2011). Our results confirm those of Rosas and Bastir (2002) and Bastir et al. (2011) who also found more upward pointing nasal bones and a downward rotation of the anterior nasal floor as common male feature in different populations. Franklin et al. (2006) yielded the same results in an indigenous southern African sample. Our results are also consistent with previous studies on linear measurements, which state that nasal height is clearly an indicator for sex while nasal breadth does not show strong discrimination between sexes (Uytterschaut, 1986; Schmittbuhl and Minor, 1998; Bastir et al., 2011; Lee et al., 2014). Discriminant analysis in our sample proved the shape of the bony nose not to be a good predictor for sex, with 69.1% correct sex classification (72.3% in Chinese and 72.7% in Germans when analyzing populations separately). Our sexing accuracy for the Germans sample is similar to that found by Bigoni et al. (2010), when taking the missing cross-validation of their results into account. However, when including centroid size as additional variable, this value raised up to 83.3% (84.6% in Chinese and 88.2% in Germans).

Additional to significant sexual dimorphism in the pooled sample, significant population specific sexual dimorphism was detected regarding the symmetric shape component. The population specific sexual

dimorphism is due to differences in specific shape characteristics rather than because of the intensity of them. In the Chinese sample, the angle of the *spina nasalis* differs slightly more between males and females than in our German sample. Because of the general population specific shape differences of the nasal bones, German male nasal bones protrude German female nasal bones in a broader region when compared to Chinese males and females. When visualized (Fig. 5), these differences between the populations appear to be subtle. This subtlety is reflected by the relatively small angle of 34.0°, indicating a similar direction of sex related shape differences in both populations. This confirms the findings of Bastir et al. (2011) who also detected population specific sexual dimorphism being only subtle (and in their case, not significant) and when pooling the samples, mainly differences in vertical direction remained.

Considering the asymmetry related to males and females, our results indicate that there is no significant difference in directional asymmetry between the sexes. Fluctuating asymmetry, on the other hand, is stronger in males than in females in both populations with no population specific differences. There is a fair amount of controversial literature on facial asymmetry, sexual attractiveness and mating strategies, especially concerning stronger fluctuating asymmetry in male faces (Grammer and Thornhill, 1994; Gangestad and Thornhill, 2003; Koehler et al., 2004; Thornhill and Gangestad, 2006; Puts, 2010). We have previously shown (Schlager, 2013) that asymmetric trends in the soft tissue nose are, to a lesser degree, also measurable in the bony nose. It is, however, beyond the scope of this study to relate our findings on sex differences in fluctuating asymmetry of the bony nose to studies on facial soft tissue. Claes et al. (2012) confirm our findings of stronger fluctuating asymmetry in males than in females in the region of the nose. This concordance encourages further investigation into the correlation between hard and soft tissue of the human nose under the aspect of sexual dimorphism and asymmetry in future studies.

## OUTLOOK

For future research regarding craniofacial asymmetry, it would be interesting to include other parts, such as the orbital region and the maxilla, in a similar detailed study to detect covariances between these functional units. Additionally, the shape of the soft tissue nose in relation to its osseous counterpart is interesting concerning the questions of airflow, the inhibited asymmetry and population specific sexual dimorphism. Future studies may involve other populations, for example from colder regions, to assess different adaptations in bony nose shape especially to cold climate. Also, detailed information on ancestry and climate would help to further investigate this aspect.

## CONCLUSION

We have focused on the bony nose and found significant shape differences between a German and a Chinese sample with a longer and slightly narrower piriform aperture in Germans, mainly induced by a steeper angle of the nasal bones at *nasion*. Also, sexual dimorphism without the influence of size differences between the sexes showed to be significant, exhibiting a more protruding and narrower bony nose in males. The use of a dense set of semi-landmarks allowed us to analyze and visualize subtle shape features that greatly extend the possibility of simple metric measurements and the geometric morphometrics based of sparsely placed landmarks. This also contributed to the analysis of asymmetry, which showed in both populations a leftward trend of the nasal bones and a trend to the right in the region of the lower part of the piriform aperture. Fluctuating asymmetry was found to be stronger in the German sample than in the Chinese and stronger in males of both populations when compared to females. While the bony nose is well suited for predicting population affinity, regarding the populations under investigation, its value for sexing unknown individuals is rather moderate. The similar expression of sexual dimorphism in those otherwise very dissimilar populations indicates common factors of these differences. We further found indications that asymmetry is also affected by the specific shape of a structure, as here the more projected features among Germans may to some degree be causing the stronger fluctuating asymmetry in this population. These insights may set yet another piece in the puzzle of human variation.

## ACKNOWLEDGMENTS

The authors would like to thank Prof. Dr. Dr. Marc Metzger from the Department of Oral and Maxillofacial Surgery, Uniklinik Freiburg, Germany, and Prof. Dr. Xianqun Fan from the Ninth People's Hospital in Shanghai for providing the CT-data. They also thank Dr. Sabrina Sholts and Dr. Sebastian Wärmländer for proof-reading and discussion and the two anonymous reviewers for their constructive comments.

## LITERATURE CITED

Adams DC, Collyer ML. 2009. A general framework for the analysis of phenotypic trajectories in evolutionary studies. Evolution 63:1143–1154.

Adams DC, Rohlf FJ, Slice DE. 2004. Geometric morphometrics: ten years of progress following the 'revolution'. Ital J Zool 71: 5–16.

Bastir M, Godoy P, Rosas A. 2011. Common features of sexual dimorphism in the cranial airways of different human populations. Am J Phys Anthropol 146:414–422.

Bastir M, Rosas A. 2013. Cranial airways and the integration between the inner and outer facial skeleton in humans. Am J Phys Anthropol 152:287–293.

Bigoni L, Veleminska J, Bruzek J. 2010. Three-dimensional geometric morphometric analysis of cranio-facial sexual dimorphism in a central german sample of known sex. Homo 61: 16–32.

Birkby WH. 1966. An evaluation of race and sex identification from cranial measurements. Am J Phys Anthropol 24:21–27.

Bookstein FL. 1989. Principal warps: thin-plate splines and the decomposition of deformations. IEEE Trans Pattern Anal Mach Intell 11:567–585.

Bookstein FL. 1997. Landmark methods for forms without landmarks: morphometrics of group differences in outline shape. Med Image Anal 1:225–243.

Boulesteix AL. 2005. A note on between-group PCA. Int J Pure Appl Math 19:359–366.

Butaric LN, McCarthy RC, Broadfield DC. 2010. A preliminary 3D computed tomography study of the human maxillary sinus and nasal cavity. Am J Phys Anthropol 143:426–436.

Claes P, Walters M, Shriver MD, Puts D, Gibson G, Clement J, Baynam G, Verbeke G, Vandermeulen D, Suetens P. 2012. Sexual dimorphism in multiple aspects of 3D facial symmetry and asymmetry defined by spatially dense geometric morphometrics. J Anat 221:97–114.

Davies A. 1932. A re-survey of the morphology of the nose in relation to climate. J R Anthropol Inst 62:337–359.
Dongen SV. 2006. Fluctuating asymmetry and developmental instability in evolutionary biology: past, present and future. J Evol Biol 19:1727–1743.
Dryden IL, Mardia KV. 1998. Statistical shape analysis. Chichester: Wiley.
Evteev A, Cardini AL, Morozova I, O'Higgins P. 2014. Extreme climate, rather than population history, explains mid-facial morphology of northern asians. Am J Phys Anthropol 153: 449–462.
Franciscus RG, Long JC. 1991. Variation in human nasal height and breadth. Am J Phys Anthropol 85:419–427.
Franklin D, Cardini A, Flavel A, Kuliukas A. 2013. Estimation of sex from cranial measurements in a western australian population. Forensic Sci Int 229:158.e1–158.e8.
Franklin D, Freedman L, Milne N, Oxnard C. 2006. A geometric morphometric study of sexual dimorphism in the crania of indigenous southern africans. S Afr J sci 102:229–238.
Gangestad SW, Thornhill R. 2003. Facial masculinity and fluctuating asymmetry. Evol Hum Behav 24:231–241.
Gilbert AN, Greenberg MS, Beauchamp GK. 1989. Sex, handedness and side of nose modulate human odor perception. Neuropsychologia 27:505–511.
Glanville EV. 1969. Nasal shape, prognathism and adaptation in man. Am J Phys Anthropol 30:29–37.
Goodall C. 1991. Procrustes methods in the statistical analysis of shape. J R Stat Soc Series B Stat Methodol 53: 285–239.
Graham JH, Raz S, Hel-Or H, Nevo E. 2010. Fluctuating asymmetry: methods, theory, and applications. 2:466–540. Symmetry
Grammer K, Thornhill R. 1994. Human (homo sapiens) facial attractiveness and sexual selection: the role of symmetry and averageness. J Comp Psychol 108:233–242.
Gunz P, Mitteroecker P. 2013. Semilandmarks: a method for quantifying curves and surfaces. Hystrix. Italian J Mammal 24:103–109.
Gunz P, Mitteroecker P, Bookstein F. 2005. Semilandmarks in three dimensions. In: Slice D, editor. Modern morphometrics in physical anthropology, developments in primatology: progress and prospects. Chicago, IL: Kluwer Academic/Plenum Publishers. p 73–98.
Harvati K, Weaver TD. 2006. Human cranial anatomy and the differential preservation of population history and climate signatures. Anat Rec 288A:1225–1233.
Hennessy RJ, McLearie S, Kinsella A, Waddington JL. 2005. Facial surface analysis by 3D laser scanning and geometric morphometrics in relation to sexual dimorphism in cerebral-craniofacial morphogenesis and cognitive function. J Anat 207:283–295.
Holton N, Yokley T, Butaric L. 2013. The morphological interaction between the nasal cavity and maxillary sinuses in living humans. Anat Rec 296:414–426.
Holton NE, Franciscus RG. 2008. The paradox of a wide nasal aperture in cold-adapted neandertals: a causal assessment. J Hum Evol 55:942–951.
Hubbe M, Hanihara T, Harvati K. 2009. Climate signatures in the morphological differentiation of worldwide modern human populations. Anat Rec 292:1720–1733.
Humphries A, Ross A. 2011. Craniofacial sexual dimorphism in two Portuguese skeletal samples. Anthropologie (Brno) 49: 13–20.
Jantz R, Ousley S. 2005. FORDISC 3: computerized forensic discriminant functions. Version 3.0. Knoxville: University of Tennessee.
Kimmerle E, Jantz R. 2005. Secular trends in craniofacial asymmetry studied by geometric morphometry and generalized Procrustes methods. In: Slice D, editors. Modern morphometrics in physical anthropology. Chicago, IL: Kluwer Academic/Plenum Publishers. p 247–263.
Kimmerle EH, Ross A, Slice D. 2008. Sexual dimorphism in america: geometric morphometric analysis of the craniofacial region. J Forensic Sci 53:54–57.
Klingenberg CP. 2003. A developmental perspective on developmental instability: theory, models and mechanisms. In: Polak M, editor. Developmental instability: causes and consequences. Oxford: Oxford University Press. p 14–34.
Klingenberg CP, Barluenga M, Meyer A. 2002. Shape analysis of symmetric structures: quantifying variation among individuals and asymmetry. Evolution 56:1909–1920.
Klingenberg CP, McIntyre GS. 1998. Geometric morphometrics of developmental instability: analyzing patterns of fluctuating asymmetry with procrustes methods. Evolution 52:1363–1375.
Koehler N, Simmons L, Rhodes M, Peters M. 2004. The relationship between sexual dimorphism in human faces and fluctuating asymmetry. Proc R Soc 271:S233–S236.
Krajícek V, Dupej J, Velemínská J, Pelikán J. 2012. Morphometric analysis of mesh asymmetry. J WSCG 20:65–72.
Langsrud Ø. 2002. 50-50 multivariate analysis of variance for collinear responses. Statistician 51:305–317.
Langsrud Ø, Jürgensen K, Ofstad R, Næs T. 2007. Analyzing designed experiments with multiple responses. J Appl Stat 34:1275–1296.
Langsrud Ø, Mevik BH. 2012. Ffmanova: fifty-fifty MANOVA. URL http://CRAN.R-project.org/package=ffmanova.
Lee K-M, Lee Dds W-J, Cho J-H, Hwang H-S. 2014. Three-dimensional prediction of the nose for facial reconstruction using Cone-beam computed tomography. Forensic Sci Int 236: 194.e1–194.e5. (0):
Mardia KV, Bookstein FL, Moreton IJ. 2000. Statistical assessment of bilateral symmetry of shapes. Biometrika 87:285–300.
Mitteroecker P, Bookstein F. 2009. The ontogenetic trajectory of the phenotypic covariance matrix, with examples from craniofacial shape in rats and humans. Evolution 63:727–737.
Mitteroecker P, Bookstein F. 2011. Linear discrimination, ordination, and the visualization of selection gradients in modern morphometrics. Evol Biol 38:100–114.
Mitteroecker P, Gunz P, Bernhard M, Schaefer K, Bookstein FL. 2004. Comparison of cranial ontogenetic trajectories among great apes and humans. J Hum Evol 46:679–697.
Mitteroecker P, Gunz P, Windhager S, Schaefer K. 2013. A brief review of shape, form, and allometry in geometric morphometrics, with applications to human facial morphology. Hystrix, the Italian J Mammal 24:59–66.
Noback ML, Harvati K, Spoor F. 2011. Climate-related variation of the human nasal cavity. Am J Phys Anthropol 145:599–614.
Özener B. 2010. Fluctuating and directional asymmetry in young human males: effect of heavy working condition and socioeconomic status. Am J Phys Anthropol 143:112–120.
Ogawa Y, Imaizumi K, Miyasaka S, Yoshino M. 2013. Discriminant functions for sex estimation of modern japanese skulls. J Forensic Leg Med 20:234–238.
Palmer AR, Strobeck C. 2003. Fluctuating asymmetry analyses revisited. In: Polak M, editor. Developmental instability: causes and consequences. Oxford: Oxford University Press. p 279–319.
Penton-Voak IS, Jones BC, Little AC, Baker S, Tiddeman B, Burt DM, Perrett DI. 2001. Symmetry, sexual dimorphism in facial proportions and male facial attractiveness. Proc Biol Sci R Soc 268:1617–1623.
Pirttiniemi P. 1998. Normal and increased functional asymmetries in the craniofacial area. Acta Odontol Scand 56: 342–345.
Puts DA. 2010. Beauty and the beast: mechanisms of sexual selection in humans. Evol Hum Behav 31:157–175. Am J Phys Anthropol
R Development Core Team. 2011. R Language Definition, version 2.132. URL http://www.r-project.org/.
Rosas A, Bastir M. 2002. Thin-plate spline analysis of allometry and sexual dimorphism in the human craniofacial complex. Am J Phys Anthropol 117:236–245.
Schlager S. 2012. Sliding semi-landmarks on symmetric structures in three dimensions. Am J Phys Anthropol 147: 261.

Schlager S. 2013. Soft-tissue reconstruction of the human nose: population differences and sexual dimorphism. PhD thesis, Universitätsbibliothek Freiburg.

Schlager S. 2014. Morpho: calculations and visualizations related to geometric morphometrics. URL http://sourceforge.net/projects/morpho-rpackage/.

Schlager S, Metzger M. 2011. Direction and intensity of sexual dimorphism in German and Chinese mandibles' outer contour. Am J Phys Anthropol 144:265.

Schmittbuhl M, Minor JL. 1998. New approaches to human facial morphology using automatic quantification of the relative positions of the orbital and nasal apertures. Surg Radiol Anat 20:321–327.

Sholts SB, Walker PL, Kuzminsky SC, Miller KWP, Wärmländer SKTS. 2011. Identification of group affinity from cross-sectional contours of the human midfacial skeleton using digital morphometrics and 3D laser scanning technology. J Forensic Sci 56:333–338.

Slice D. 2005. Modern morphometrics. In: Slice D, editor. Modern morphometrics in physical anthropology. Chicago, IL: Kluwer Academic/Plenum Publishers. p 1–45.

Thomson A, Buxton LHD. 1923. Man's nasal index in relation to certain climatic conditions. J R Anthropol Inst 53: 92–122.

Thornhill R, Gangestad S. 2006. Facial sexual dimorphism, developmental stability, and susceptibility to disease in men and women. Evol Hum Behav 27:131–144.

Uytterschaut H. 1986. Sexual dimorphism in human skulls. A comparison of sexual dimorphism in different populations. Hum Evol 1:243–250.

Yokley T. 2009. Ecogeographic variation in human nasal passages. Am J Phys Anthropol 138:11–22.